Catalysis Communications 177 (2023) 106633

Contents lists available at ScienceDirect

Catalysis Communications

journal homepage: www.elsevier.com/locate/catcom

Mechanistic kinetic modeling of the rhodium-catalyzed tandem hydroaminomethylation of 1-decene in a thermomorphic solvent system

Wieland Kortuz [a,b,*], Sabine Kirschtowski [b], Andreas Seidel-Morgenstern [a], Christof Hamel [b]

[a] Max Planck Institute for Dynamics of Complex Technical Systems Magdeburg, Sandtorstraße 1, 39106 Magdeburg, Germany
[b] Otto von Guericke University Magdeburg, Institute of Process Engineering, Universitätsplatz 2, 39106 Magdeburg, Germany

ARTICLE INFO

Keywords:
Homogeneous rhodium catalysis
Hydroaminomethylation
Tandem reaction
Thermomorphic solvent system
Catalytic cycle
Mechanistic kinetic modeling

ABSTRACT

For a more resource-efficient production of amines the homogeneously catalyzed tandem hydroaminomethylation reaction is of large relevance. The kinetics of the sulfoxantphos-rhodium-catalyzed hydroaminomethylation of 1-decene were studied exploiting a thermomorphic solvent system. Focus was a mechanistic kinetic description of the enamine hydrogenation as the final step in the tandem reaction. Based on proposing a catalytic cycle and applying the Christiansen mathematics, a mechanistic rate model was derived and parameterized. The mechanistic model was able to describe the experimental observations in a broad range of operation conditions including pressure and temperature perturbations providing the basis for process design and optimization.

1. Introduction

Homogeneous catalysis offers large potential to develop new resource-efficient processes. The usage of transition metals like rhodium in combination with bidentate ligands enables the design of highly active and selective catalysts [1,2]. The advantage of homogeneously catalyzed reactions such as the hydroaminomethylation (HAM) is the absence of resistances of the mass transfer in the fluid phase to the dissolved catalyst. This advantage is connected with the often challenging need to separate the catalyst from the reaction mixture in order to recycle it. This is especially the case when costly metals like rhodium are used. The collaborative research center "Integrated Chemical Processes in Liquid Multiphase Systems" (InPROMPT) explored several catalyst recycling strategies with a focus on switchable solvent systems, recently summarized in Kraume et al. [3]. One of the attractive options is the application of mixtures of solvents, which form a thermomorphic solvent system (TMS) [4–7]. The temperature dependency of the miscibility of the constituents is used to switch between a reaction mode (one phase) and a separation mode (two phases). The operation principle is illustrated in Fig. S1 in the supporting information. To apply the concept, at least one polar and one unpolar solvent are needed which are characterized by a miscibility gap at a lower temperature level. At higher temperatures a homogeneous phase is formed and the reaction can take place without mass transfer limitations in the fluid phase. To recover the catalyst, the mixture is cooled down to trigger the phase separation. Catalyst and product are present in different phases to allow for separation. The functionality of TMS can be further increased by adding components that act as solvent mediators [4–7].

On the way to a more sustainable economy the utilization of renewable resources for established processes in the chemical industry is a major goal. The concept of TMS can be a helpful tool for harnessing those feedstocks [3,8–10]. In addition to catalyst recycling strategies new reactor concepts [11,12] and real process influences like impurities [13] were explored within InPROMPT. First, the synthesis of molecules with oxygen containing functionalities from alkenes were investigated [3]. Afterwards, the implementation of a nitrogen functionality was studied in a second consecutive step.

Amines have broad applications. They are used e.g. as agrochemicals, pharmaceuticals, dyes and detergents. Classic amine synthesis is performed through multiple reaction and separation steps in between several process steps. The application of a tandem reaction could decrease significantly the apparative effort. In addition, there is potential that byproduct formation from intermediates, being very sensitive to side reactions, is decreased due to their lower concentration compared to multi-pot synthesis [14,15]. The HAM, performed in a TMS, is characterized as a homogeneously catalyzed tandem reaction converting alkenes in a one-pot synthesis to amines [6]. The first reaction step is the hydroformylation (Hyfo) to aldehydes (terminal, branched) with

* Corresponding author at: Max Planck Institute for Dynamics of Complex Technical Systems Magdeburg, Sandtorstraße 1, 39106 Magdeburg, Germany.
E-mail address: kortuz@mpi-magdeburg.mpg.de (W. Kortuz).

https://doi.org/10.1016/j.catcom.2023.106633
Received 16 January 2023; Received in revised form 27 February 2023; Accepted 28 February 2023
Available online 5 March 2023

synthesis gas. Afterwards a reductive amination (RA) takes place. It comprises an equilibrium-limited condensation reaction with a co-substrate amine to form the enamine followed by its hydrogenation to the product amine (Fig. 1). Hyfo and enamine hydrogenation are catalyzed reactions. Side reactions occur, but water is the only co-product formed in the condensation reaction step. This is a major advantage of this reaction pathway compared to other ones generating unwanted toxic or environmentally dangerous co-products [16,17]. The rhodium-sulfoxantphos-catalyzed HAM of the model substrate 1-decene in a TMS consisting of methanol (MeOH) and n-dodecane (Dod) is investigated experimentally by instructive perturbation experiments in particular to study the influence of water on the chemical equilibrium. This data forms the basis for a detailed mechanistic kinetic modeling of the reactions involved.

For process design and optimization reliable mathematical models are required. Thus, the description of the reaction kinetics is a key issue. Simple power law kinetics are often valid in a very limited operation window. Including knowledge about the reaction mechanism can increase the extrapolability and transferability of the model. In this contribution a mechanistic model description of the reaction rate of the enamine hydrogenation is derived and an existing kinetic approach for the HAM [15] with the Hyfo [10] as initial reaction step is adjusted accordingly.

2. Experimental

A description of the experimental setup, the reaction network with all side reactions and its reduction to the components and reactions with significance as illustrated in Fig. 2 can be found in preliminary studies [15]. The used chemicals and their purities can be found in Table S1 in the supporting information. New instructive perturbation experiments including the analytics follow the procedure and methodology described in [15]. Table S2 in the supporting information summarizes results of these experiments with respect to the conversion of the substrate $X_{1\text{-dec}}$ and the yield of the target product n-amine Y_{am}. All experiments were conducted as semi-batch experiments in a stirred, stainless steel tank reactor with dosing of the gaseous reactants via a pressure regulator. 1-decene is used as model substrate in combination with diethylamine (DEA) as co-substrate for the enamine formation. The catalyst in resting state is formed during the preforming with synthesis gas from the pre-catalyst Rh(acac)(COD) and the ligand sulfoxantphos. The TMS is composed of 50 wt% MeOH and 50 wt% Dod.

The HAM consists of the Hyfo followed by the RA and their side reactions [10,14,18,19]. The most dominant side reaction is the isomerization (Iso) of the terminal alkene to linear isomers with an internal double bond. These are lumped together as a pseudo-component isodecene [18,20,21]. The hydrogenation of 1-decene to n-decane (Hyd,1-dec) is the second relevant side reaction considered in the modeling. Alcohol and aldol formation classically decreasing the amine selectivity in RA processes are negligible in the tandem reaction due to the low concentration of the aldehyde and the enamine observed in the experiments. The reaction network including the isomerization (r_{Iso}) and hydrogenation of 1-decene ($r_{Hyd,1-dec}$) depicted in Fig. 2 contains 10 components, 2 reversible and 3 irreversible reactions.

3. Kinetic description and modeling of the tandem hydroaminomethylation

For a mechanistic kinetic description and modeling of the homogeneously catalyzed tandem reaction HAM detailed knowledge about the underlying reaction mechanisms in particular of the catalytic cycles is required. With this knowledge Christiansen mathematics can be applied to derive rate equations. This was done in preliminary work for the Hyfo and its side reactions [10,18,21] and will be done in this contribution for the hydrogenation of the enamine as the final reaction step of the tandem HAM to improve a previously used power law based kinetic model [15].

3.1. Subnetwork hydroformylation, isomerization and hydrogenation of 1-decene

The proposed elementary reaction sequences including assumptions about irreversible steps and the abundance of catalytic species of the catalyzed reactions were adopted according to Jörke et al. for the Hyfo subnetwork including isomerization and hydrogenation of 1-decene. Thus, these rate equations (Eqs. (1–3)) were applied as published before, even though another bidentate ligand (BiPhePhos) and TMS (DMF, n-decane) were used [10,15,21]. Jameel et al. found only minor differences of the Gibbs free energies for the Hyfo going from DMF to MeOH and no change in the elementary reaction sequence using DFT calculations [22].

$$r_{Hyfo} = \frac{k_{Hyfo} \cdot c_{1-dec} \cdot c_{CO} \cdot c_{H_2} \cdot c_{cat}}{1 + K^{I}_{Hyfo} \cdot c_{H_2} + K^{II}_{Hyfo} \cdot c_{CO} \cdot c_{H_2}} \tag{1}$$

$$r_{Hyd,1-dec} = \frac{k_{Hyd,1-dec} \cdot c_{1-dec} \cdot c_{H_2} \cdot c_{cat}}{1 + K_{Hyd,1-dec} \cdot c_{H_2}} \tag{2}$$

$$r_{Iso} = \frac{k_{Iso} \cdot \left(c_{1-dec} - \frac{c_{i-dec}}{K^{eq}_{Iso}} \right) \cdot c_{cat}}{1 + K^{II}_{Iso} \cdot c_{i-dec}} \tag{3}$$

3.2. Subnetwork condensation

The condensation reaction to form the enamine from the aldehyde with DEA is equilibrium-limited. It connects the Hyfo subnetwork and the subsequent enamine hydrogenation. This reaction is the only one in the modeled network (Fig. 2) which proceeds at reaction conditions without rhodium catalyst as observed in preliminary experiments. An influence of the catalyst on the reaction kinetics of the condensation reaction is not assumed [17,23]. The following rate equation (Eq. (4)) is adopted from Kirschtowski et al. [14,15].

$$r_{Cond} = k_{Cond} \cdot \left(c_{und} \cdot c_{DEA} - \left(\frac{c_{en} \cdot c_{H_2O}}{K^{eq}_{Cond}} \right) \right) \tag{4}$$

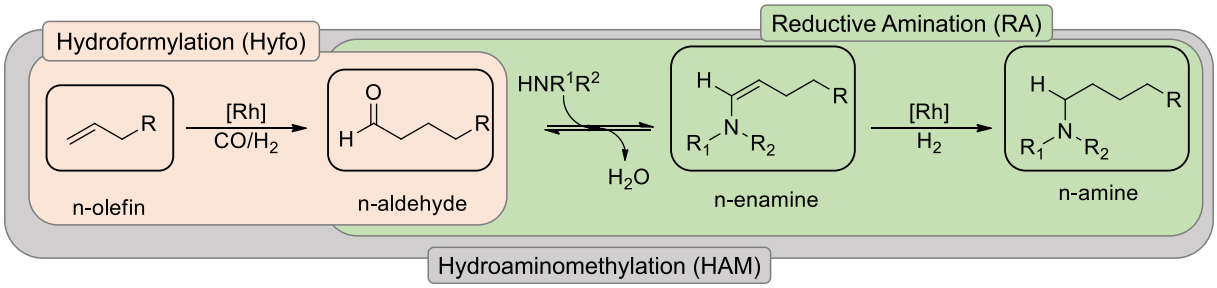

Fig. 1. Main reaction pathway of the HAM consisting of Hyfo and RA.

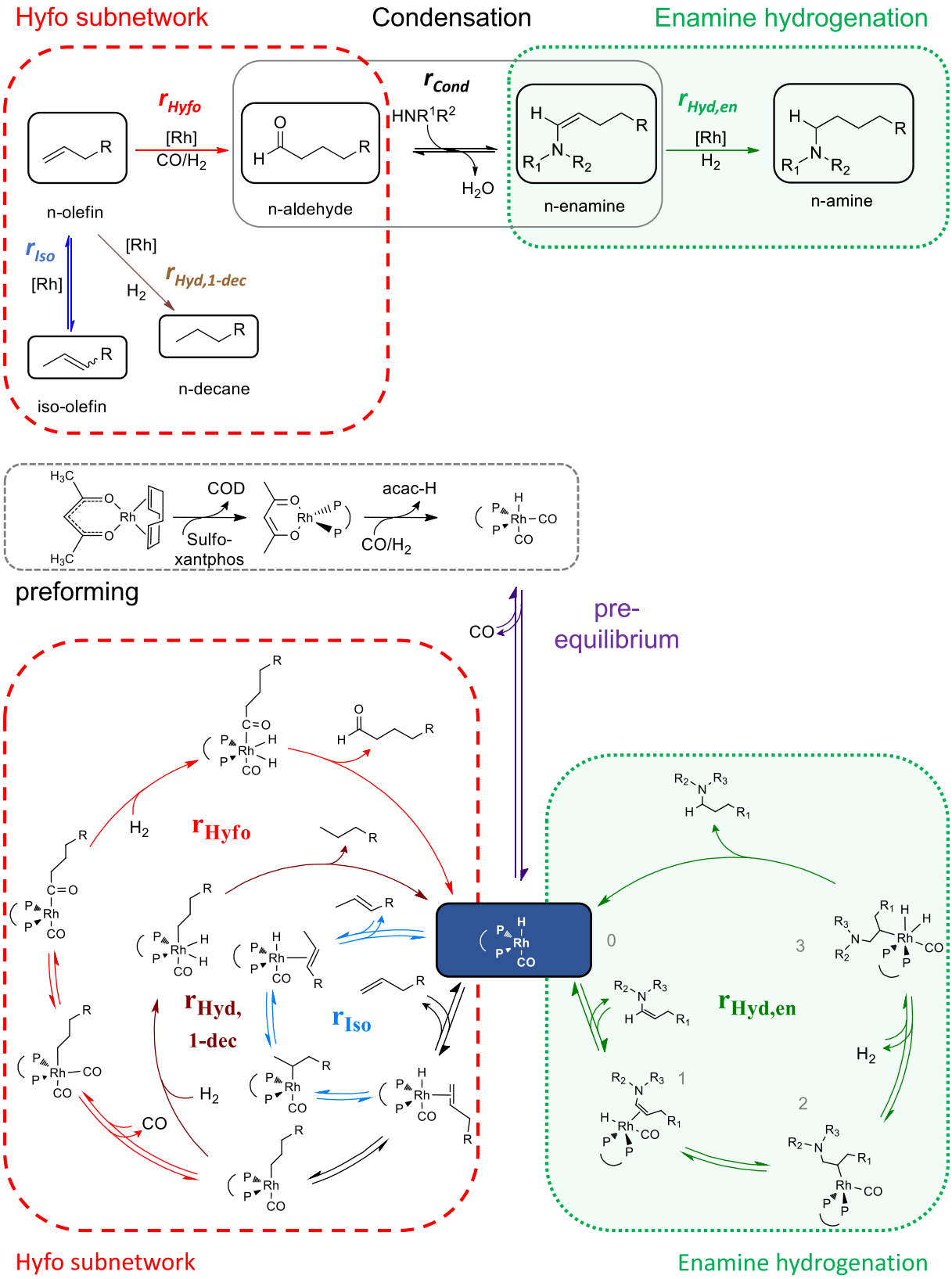

Fig. 2. Reaction network and catalytic cycles of the HAM of a n-olefin (Hyfo + RA) with major side reactions (isomerization and substrate hydrogenation).

3.3. Subnetwork hydrogenation of the enamine

The usage of *operando* FTIR for analyzing the catalytic species is not possible due to the presence of DEA in the HAM system which would corrode the silica probe in short time. Therefore, the underlying catalytic cycle for the enamine hydrogenation could not be determined in own experimental studies in contrast to the Hyfo before. Several authors deviate in their assumptions about the active catalyst species, the

sequence of the elementary reaction steps and which of them being rate-determining for the enamine or imine hydrogenation in the RA and within the tandem reaction HAM using different substrates, solvents and catalytic systems [17,24–27]. The elementary reaction sequence contains the coordination of the enamine to the metal center, insertion to the Rh-H-bond, the oxidative addition of dihydrogen and the reductive elimination of the amine [23,28]. Crozet et al. suggest this sequence according to their DFT calculations of Gibbs free energy profiles for the HAM of styrene with piperidine in THF using a rhodium catalyst in combination with a diphosphine ligand [28]. Jameel et al. determine the same order of the elementary steps for the hydrogenation of the enamine in the RA of undecanal with DEA in a TMS consisting of MeOH/Dod with pure hydrogen in the gas phase [26]. In the Hyfo a monocarbonyl hydrid complex acts as active catalytic species which is gained when the dicarbonyl hydrid species resting state frees a coordination site by releasing a carbonyl group. Crozet et al. assume according to their findings in NMR experiments that this complex is the active species for the enamine hydrogenation during HAM conditions with CO present [28]. This assumption leads to the catalytic cycle postulated in Fig. 2 [28]. For the hydrogenation of the enamine no significant back reaction can be observed experimentally. Thus, at least one of the elementary steps of the catalytic cycle is irreversible, which is the final product elimination assumed to be according to the Hyfo [10]. An important commonality between the system investigated by Crozet et al. and this contribution is the presence of CO which can have a crucial influence on the active catalytic species of a hydrogenation [29,30]. CO is a strong binding ligand at the rhodium center [28]. Therefore, the active catalytic species is probably not the same when synthesis gas is applied as gas phase compared to pure hydrogen. The RA expires also in the presence of CO. Therefore, it is assumed according to Crozet et al. that the active catalytic species during HAM is the same for Hyfo and RA [28]. Assumptions are based on literature where similar but different systems regarding the applied substrate, catalyst ligands and solvents were investigated. These differences are assumed to influence the activation energies of the elementary reaction steps but not the mechanism itself.

On the basis of the catalytic cycle rate equations can be derived using Christiansen mathematics [31–33]. This approach is an algorithm applying Bodenstein's quasi-steady-state assumption for all catalytic species and elementary steps. Therefore, requirements need to be fulfilled. Consequently, all concentrations of the catalytic species have to stay at trace level ensuring that no accumulation occurs neglecting a short initial period which justifies the quasi-steady-state assumption. Furthermore, no intermediate of the catalytic cycle is allowed to react with another one enabling a pseudo-first order description of all elementary reactions which leads to the advantage that only linear algebra is necessary. Of course, the catalytic species are allowed to react with educts which are not catalytic intermediates themselves. The concentration of these co-reactants c_i and the actual reaction rate coefficient k are combined to a pseudo-first order rate coefficient λ (Eq. (5)).

$$\lambda_{m,m+1} = k_{m,m+1} \cdot \prod_{i=1}^{N_{com}} c_i^{(-\nu_i)} \tag{5}$$

Several authors already described how to construct the Christiansen matrix C depending on the number of intermediates in the catalytic cycle and how to reduce it considering irreversible and rate-determining elementary reaction steps or most/low abundant species [3,10,18,31,32]. Every row of the matrix C corresponds to the concentration of one intermediate of the catalytic cycle. A general formulation of the rate approach r_P contains all forward and backward pseudo-first order rate coefficients combined with the active catalyst concentration c_{cat} in the numerator and the sum of all entries of the reduced Christiansen matrix CS in the denominator (Eq. (6)).

$$r_P = \frac{\left[\prod_{m=0}^{M-1} \lambda_{m,m+1} - \prod_{m=0}^{M-1} \lambda_{m+1,m}\right] \cdot c_{cat}}{CS} \tag{6}$$

If at least one elementary step of the catalytic cycle is irreversible the whole reaction sequence is irreversible and the product of the backward pseudo-first order rate coefficients in the numerator becomes zero.

The catalytic cycle of the enamine hydrogenation contains four intermediates (0, 1, 2, 3) starting with the monohydride monocarbonyl catalyst species as illustrated in Fig. 2. The Christiansen matrix is a square matrix. The number of rows equals the number of intermediates of the catalytic cycle. For this case the Christiansen matrix (Eq. (7)) can be formulated as follows.

$$C = \begin{bmatrix} \lambda_{12}\lambda_{23}\lambda_{30} & \lambda_{10}\lambda_{23}\lambda_{30} & \lambda_{10}\lambda_{21}\lambda_{30} & \lambda_{10}\lambda_{21}\lambda_{32} \\ \lambda_{23}\lambda_{30}\lambda_{01} & \lambda_{21}\lambda_{30}\lambda_{01} & \lambda_{21}\lambda_{32}\lambda_{01} & \lambda_{21}\lambda_{32}\lambda_{03} \\ \lambda_{30}\lambda_{01}\lambda_{12} & \lambda_{32}\lambda_{01}\lambda_{12} & \lambda_{32}\lambda_{03}\lambda_{12} & \lambda_{32}\lambda_{03}\lambda_{10} \\ \lambda_{01}\lambda_{12}\lambda_{23} & \lambda_{03}\lambda_{12}\lambda_{23} & \lambda_{03}\lambda_{10}\lambda_{23} & \lambda_{03}\lambda_{10}\lambda_{21} \end{bmatrix} \tag{7}$$

The first row of the Christiansen matrix is obtained from another square matrix D (Eq. (8)) with ones at the diagonal and the forward pseudo-first order rate coefficients above and the backward pseudo-first order rate coefficients below the diagonal. Each column corresponds to one elementary step of the catalytic cycle.

$$D = \begin{bmatrix} 1 & \lambda_{12} & \lambda_{23} & \lambda_{30} \\ \lambda_{10} & 1 & \lambda_{23} & \lambda_{30} \\ \lambda_{10} & \lambda_{21} & 1 & \lambda_{30} \\ \lambda_{10} & \lambda_{21} & \lambda_{32} & 1 \end{bmatrix} \tag{8}$$

The product of the entries of each row of this matrix D is one element in the first row of the Christiansen matrix C. The following rows are derived from the previous one. Every index increases by one and the highest index becomes zero. From the last row the first one can be constructed in the same way.

According to the Hyfo reaction network it was assumed that the monohydride monocarbonyl catalyst species is the only one present in significant amounts. Therefore, it is called the most abundant catalyst containing species (macs). When only this species is dominant, the other rows of the Christiansen matrix corresponding with the minor species become negligible. This allows an impactful reduction of the Christiansen matrix and number of kinetic parameters, respectively.

$$C = \begin{bmatrix} \lambda_{12}\lambda_{23}\lambda_{30} & \lambda_{10}\lambda_{23}\lambda_{30} & \lambda_{10}\lambda_{21}\lambda_{30} & \lambda_{10}\lambda_{21}\lambda_{32} \\ 0 & 0 & 0 & 0 \\ 0 & 0 & 0 & 0 \\ 0 & 0 & 0 & 0 \end{bmatrix} \tag{9}$$

By applying Eqs. (6,9) and considering the assumption of irreversibility of the enamine hydrogenation coinciding with the experimental observations the following rate approach (Eq. (10)) is obtained.

$$r_{Hyd,en} = \frac{\lambda_{01}\lambda_{12}\lambda_{23}\lambda_{30} \cdot c_{cat}}{\lambda_{12}\lambda_{23}\lambda_{30} + \lambda_{10}\lambda_{23}\lambda_{30} + \lambda_{10}\lambda_{21}\lambda_{30} + \lambda_{10}\lambda_{21}\lambda_{32}} \tag{10}$$

It still contains the pseudo-first order rate coefficients which will be substituted in the next steps.

$$\begin{aligned} &\lambda_{01} = k_{01} \cdot c_{en}; \lambda_{12} = k_{12}; \lambda_{23} = k_{23} \cdot c_{H_2}; \lambda_{30} = k_{30}; \\ &\lambda_{10} = k_{10}; \lambda_{21} = k_{21}; \lambda_{32} = k_{32}; \lambda_{03} = k_{03} \cdot c_{am} \end{aligned} \tag{11}$$

$$r_{Hyd,en} = \frac{k_{01}k_{12}k_{23}k_{30} \cdot c_{en} \cdot c_{H_2} \cdot c_{cat}}{k_{12}k_{23}k_{30} \cdot c_{H_2} + k_{10}k_{23}k_{30} \cdot c_{H_2} + k_{10}k_{21}k_{30} + k_{10}k_{21}k_{32}} \tag{12}$$

Lumping the constants together the following expression is derived.

$$r_{Hyd,en} = \frac{k_{Hyd,en} \cdot c_{en} \cdot c_{H_2} \cdot c_{cat}}{1 + K_{Hyd,en} \cdot c_{H_2}} \text{ with} \tag{13}$$

$$k_{Hyd,en} = \frac{k_{01}k_{12}k_{23}k_{30}}{k_{10}k_{21}(k_{30}+k_{32})} \text{ and}$$
$$K_{Hyd,en} = \frac{k_{23}k_{30}(k_{12}+k_{10})}{k_{10}k_{21}(k_{30}+k_{32})} \quad (14)$$

The new mechanistic rate approach for the enamine hydrogenation (Eq. (13)) has only one more parameter than a simple power law approach with simultaneously improved validity [15].

The reaction between the resting state and the active catalyst species is assumed to be in equilibrium proceeding significantly faster than the other reactions [10,18]. The rate effecting concentration of the active catalyst c_{cat} is dependent on the total amount of catalyst and the solubilized concentration of CO.

$$c_{cat} = \frac{c_{cat,tot}}{1 + K_{cat}^{eq} \cdot c_{CO}} \quad (15)$$

3.4. Reactor model

As described in chapter 2 the experiments were performed applying semi-batch operation. The change of the concentrations for the liquid components over time is due to the reactions j.

$$\frac{dc_i}{dt} = \sum_{j=1}^{N_j} (\nu_{i,j} \cdot r_j) \quad (16)$$

An additional mass transport term from the gas into the liquid phase is necessary for the description of the gaseous substances. It includes an effective mass transfer coefficient β_{eff} and the saturation concentration c^*.

$$\frac{dc_i}{dt} = \beta_{eff,i} \cdot (c_i^* - c_i) + \sum_{j=1}^{N_j} (\nu_{i,j} \cdot r_j) \quad (17)$$

The Arrhenius approach is used to model the temperature dependency of the reaction rate constant.

$$k_j = k_{0,j} \cdot e^{-\frac{E_{A,j}}{RT}} \quad (18)$$

3.5. Results and discussion of the parameter estimation

For the collision factor, the activation energy and the new mechanistic constant $K_{Hyd,en}$ (Eq. (13)) of the final hydrogenation step a new parameter estimation was done. The kinetic parameters of the other reactions (r_{Hyfo}; $r_{Hyd,1-dec}$; r_{Iso}; r_{Cond}) did not change significantly when all parameters were estimated together indicating that they are already sufficient to describe these reactions. This is why those parameters were kept constant in a second step and only the parameters of the enamine hydrogenation were estimated newly. This leads to a number of three free parameters shown in Eq. (19).

$$\Theta = [\, k_{0,Hyd,en} \quad E_{A,Hyd,en} \quad K_{Hyd,en} \,] \quad (19)$$

As objective function (OF) the sum of the absolute differences between the experimental and simulated concentration values for all components, experiments and samples was used. It was minimized by the lsqnonlin solver integrated in *MATLAB*®.

$$OF = \sum_{i=1}^{N_{com}} \sum_{ex=1}^{N_{ex}} \sum_{sam=1}^{N_{sam}} \left| c_{i,ex,sam}^{mod} - c_{i,ex,sam}^{exp} \right| \quad (20)$$

The experimental basis for the parameter estimation is the same as for the not fully mechanistic model published in [15]. The new perturbation experiments of this contribution are used for evaluation only. The estimated activation energy of the enamine hydrogenation $E_{A,Hyd,en}$ is 18.32 kJ/mol being in the same order of magnitude compared to the previously published activation energy with a power law model of 24.82 kJ/mol [15]. This is in accordance with the fact that the temperature dependency which is expressed by the activation energy does not change when going from a power law model to a mechanistic description. For the mechanistic constant $K_{Hyd,en}$ in the denominator of Eq. (13) a value of 6.49 L/mol is obtained allowing a better consideration of the hydrogen influence on the reaction rate. The collision factor is with $1.5487 \cdot 10^9$ $L^2/mol^2/min$ as well in the same range as the one from the power law model [15]. The supporting information contains the estimated values with their confidence intervals in Table S3 and the constant parameters during parameter estimation summarized in Table S4.

3.6. Model evaluation including perturbation experiments

The influence of the temperature on the reaction kinetics is depicted in Fig. 3a for the substrate and the product n-amine as well as for the side products isodecene and n-decane in Fig. 3b. The new model is able to describe the performed semi-batch experiments successfully.

Water as co-product promotes the backward reaction of the equilibrium-limited condensation reaction as illustrated in Fig. 2. After the phase separation of the TMS most of the water will be in the polar phase which will be recycled [6]. Therefore, an accumulation of water is a realistic scenario in a continuous production process and thus its kinetic influence is of special interest [34]. The trend of the influence of the initial water amount on the HAM reaction kinetics can be described by the new model sufficiently (Fig. 3c) even though the effect is very small in the investigated range realizing a homogeneous condition. The presence of water has a significant influence on the phase behavior of the TMS and increases the required temperature to achieve one homogeneous liquid phase [34,35]. Therefore, only experiments up to 1 vol% of initial water were conducted to ensure that only one liquid phase is present at reaction conditions. Otherwise, the model would not be applicable to cover the distribution of all components in two different liquid phases. Phase calculations to ensure monophasic liquid conditions would be beneficial. The results shown in Fig. 3c indicate that a higher initial water amount has no effect on the reaction kinetics of the Hyfo, but the condensation reaction step affects the n-amine formation. The deviation of the experimental results for the substrate 1-decene is in the range of the experimental error (Fig. 3c). The same holds for the not depicted concentration profiles of the side products isodecene and n-decane. Thus, a promotional effect of water on the Hyfo as described in Chen et al. is not observed in the investigated operation regime [36]. From the absence of an influence of water on the Hyfo it is concluded that water does not significantly interferes with the rhodium catalytic species like reported for the hydroxycarbonylation supporting the proposed reaction mechanism in Fig. 2 [37].

To evaluate the new mechanistic kinetic model a dynamic experiment with a temperature and pressure perturbation has been conducted (see Fig. 4). The concentration profiles can be predicted with good accuracy for the substrate 1-decene, the main product n-amine and the side products isodecene and n-decane revealing the broad application range of the model.

4. Conclusions and outlook

This contribution focuses on kinetic modeling of the homogeneously sulfoxantphos-rhodium- catalyzed hydroaminomethylation of 1-decene performed experimentally in a thermomorphic solvent system. On the basis of a postulated catalytic cycle for the enamine hydrogenation a new mechanistic rate model was derived and combined with previously suggested mechanistic rate equations for the hydroformylation step including isomerization and hydrogenation of the olefin. With the help of the Christiansen approach a mathematical kinetic description was constructed taking the intermediate catalyst species and elementary reactions into account. Based on this mechanistic information and experimental observations, a model reduction was performed. An estimation of the kinetic parameters of the enamine hydrogenation led to an overall mechanistic model capable to describe in a broad range the

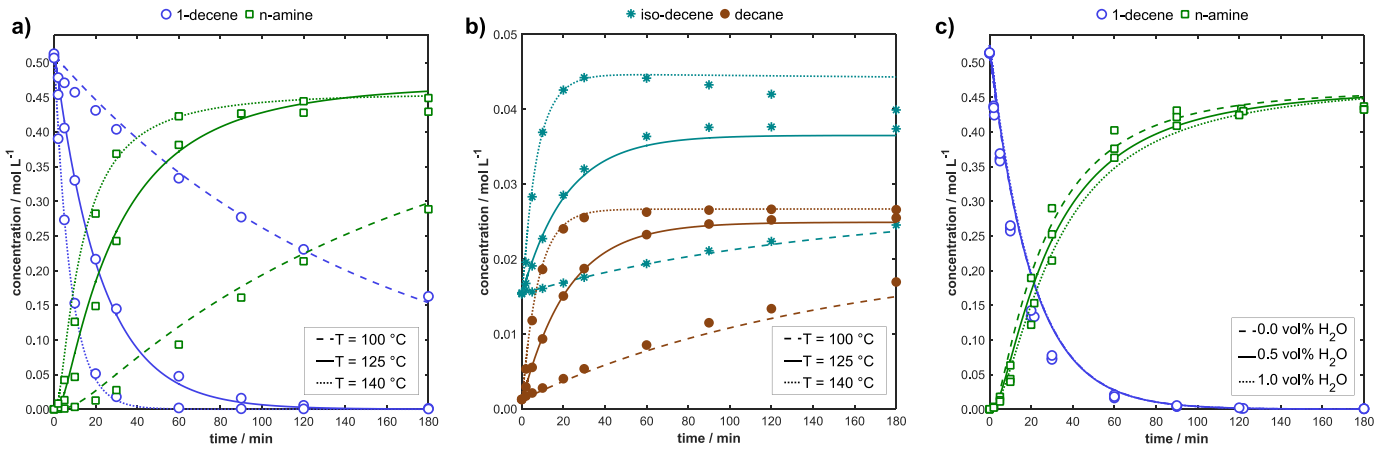

Fig. 3. Simulation (lines) and experimental (symbols) results for semi-batch experiments for the HAM of 1-decene, conditions: $p_{preforming} = 10$ bar; $CO:H_2 = 1:2$; $x_{cat} = 0.08$ mol%; $Rh/L = 1:3.5$; $w_{1\text{-dec},0} = 10$ wt%; $n_{DEA,0}/n_{1\text{-dec},0} = 8:7$; MeOH/Dod = 50:50 wt%; a) temperature influence on 1-decene & n-amine ($p_{reaction} = 45$ bar), b) temperature influence on isodecene & n-decane ($p_{reaction} = 45$ bar), c) influence of the initial water amount on 1-decene & n-amine ($T = 125$ °C; $p_{reaction} = 30$ bar).

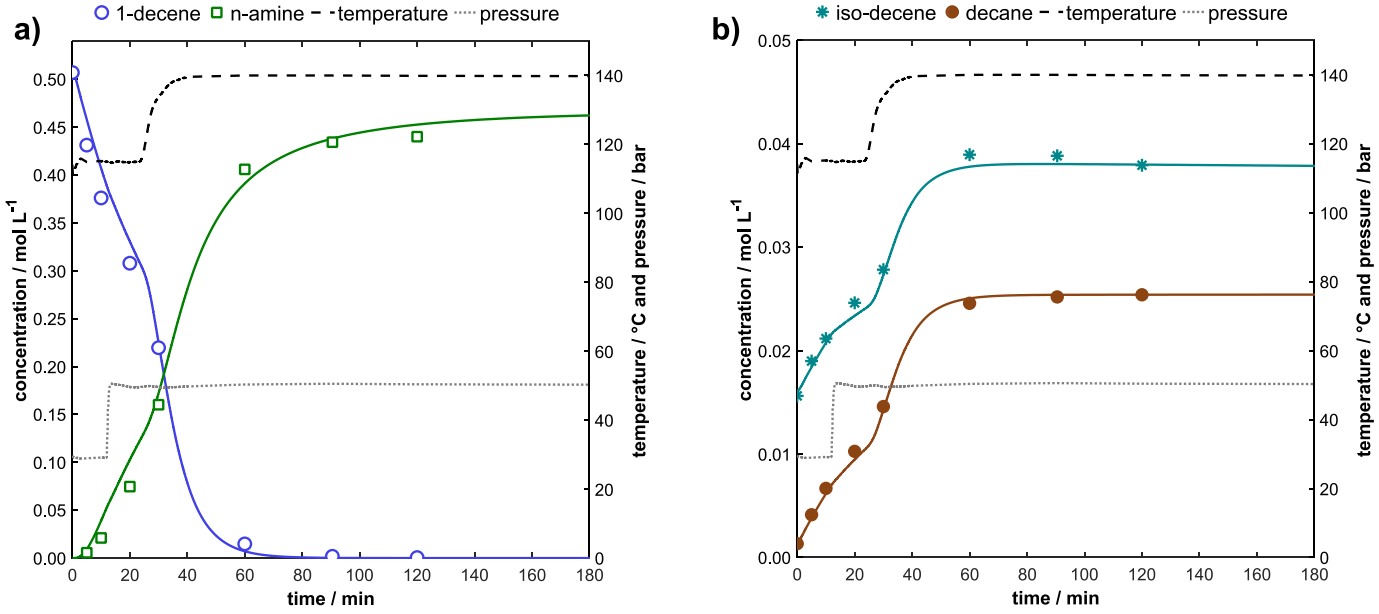

Fig. 4. Simulation (lines) and experimental (symbols) results for a perturbation experiment for the HAM of 1-decene, conditions: $T = 115$–140 °C; $p_{reaction} = 30$–50 bar; $p_{preforming} = 10$ bar; $CO:H_2 = 1:2$; $x_{cat} = 0.08$ mol%; $Rh/L = 1:3.5$; $w_{1\text{-dec},0} = 10$ wt%; $n_{DEA,0}/n_{1\text{-dec},0} = 8:7$; MeOH/Dod = 50:50 wt%; a) 1-decene & n-amine, b) isodecene & n-decane.

influence of pressure and temperature perturbations for the total network of the tandem HAM reaction. Hereby, previously reported kinetic parameters of the hydroformylation subnetwork and the condensation reaction could be kept constant indicating their quality. The overall model provides a reliable basis for process modeling, design and optimization. The transfer of this model structure to similar systems with other substrates, catalyst ligands and solvents is possible, if the reaction mechanism does not change. The kinetic parameters must be re-evaluated critically and adjusted if necessary.

The impact of the gas composition at low partial pressures on the reaction kinetics is still challenging. For a sufficient description of the complex interaction between the catalyst pre-equilibrium and gas transfer effects an improved model on a mechanistic basis which was developed in this contribution as well as an optimal experimental design are required. The latter is part of ongoing work. Due to uncertainties concerning the phase behavior increasing the initial water amount experiments on the water influence were only done in a limited range. Thus, reliable phase calculations should be embedded in a future experimental design.

Symbols

c	molar concentration [mol L^{-1}]
C	Christiansen matrix [min^{1-M}]
CI	confidence interval [variable]
CS	sum of all entries of the Christiansen matrix [min^{1-M}]
D	matrix for first row of C
E_A	activation energy [J mol^{-1}]
k	reaction rate constant [L^{q-1} $mol^{-(q-1)}$ min^{-1}]
k_0	collision factor [L^{q-1} $mol^{-(q-1)}$ min^{-1}]
K	mechanistic constant [variable]
K^{eq}	equilibrium constant [-]
M	total number of species in catalytic cycle [-]
N	total number [-]
OF	objective function [mol L^{-1}]
p	pressure [bar]

q	reaction order [-]
r	reaction rate [mol L^{-1} min^{-1}]
R	universal gas constant [J mol^{-1} K^{-1}]
Rh/L	molar rhodium ligand ratio [mol mol^{-1}]
t	time [min]
T	temperature [°C] or [K]
w	mass fraction [wt%]
x	molar fraction [mol%]

Greek letters

β_{eff}	effective mass transfer coefficient [min^{-1}]
Θ	parameter vector
λ	pseudo-first order rate coefficient [min^{-1}]
ν	stoichiometric coefficient [-]
Φ	volume fraction [vol%]

Sub- and superscripts

*	saturation
I, II	numbering of constants
0	initial condition
1-dec	1-decene
am	n-amine
cat	catalyst
CO	carbon monoxide
com	component
Cond	condensation
DEA	diethylamine
en	n-enamine
ex	experiment index
exp	experimental data
H_2	hydrogen
H_2O	water
Hyd,1-dec	hydrogenation of 1-decene
Hyd,en	hydrogenation of n-enamine
i	component index
i-dec	isodecene
Iso	isomerization
j	reaction index
m	catalytic species index
mod	modeled data
P	product
preforming	before reaction
reaction	after substrate is added
sam	sample index
tot	total
und	undecanal (aldehyde)

Abbreviations

acac	acetylacetonato
COD	1,5-cyclooctadiene
DEA	diethylamine
DFG	German Science Foundation
DFT	density functional theory
DMF	dimethylformamide
Dod	n-dodecane
FTIR	Fourier-transform infrared spectroscopy
HAM	hydroaminomethylation
Hyfo	hydroformylation
InPROMPT	Integrated Chemical Processes in Liquid Multiphase Systems
macs	most abundant catalyst containing species
MeOH	methanol
NMR	nuclear magnetic resonance
OF	objective function
RA	reductive amination
THF	tetrahydrofuran
TMS	thermomorphic multiphase solvent system

CRediT authorship contribution statement

Wieland Kortuz: Conceptualization, Methodology, Software, Formal analysis, Investigation, Visualization, Writing - original draft. **Sabine Kirschtowski:** Methodology, Validation, Investigation, Data curation, Writing – review & editing, Visualization. **Andreas Seidel-Morgenstern:** Resources, Writing – review & editing, Supervision, Funding acquisition. **Christof Hamel:** Conceptualization, Methodology, Writing – review & editing, Supervision, Project administration, Funding acquisition.

Declaration of Competing Interest

The authors declare that they have no known competing financial interests or personal relationships that could have appeared to influence the work reported in this paper.

Data availability

Data will be made available on request.

Acknowledgment

Gefördert durch die Deutsche Forschungsgemeinschaft (DFG) - TRR 63 “Integrierte chemische Prozesse in flüssigen Mehrphasensystemen” (Teilprojekt A3) - 56091768. Funded by the Deutsche Forschungsgemeinschaft (DFG, German Research Foundation) - TRR 63 “Integrated Chemical Processes in Liquid Multiphase Systems” (subproject A3) - 56091768.

This work is also part of the research initiative “SmartProSys: Intelligent Process Systems for the Sustainable Production of Chemicals” funded by the Ministry for Science, Energy, Climate Protection and the Environment of the State of Saxony-Anhalt.

We acknowledge support by the Open Access Publication Fund of Magdeburg University.

We are grateful for the supply of the catalyst precursor from Umicore.

Appendix A. Supplementary data

Supplementary data to this article can be found online at https://doi.org/10.1016/j.catcom.2023.106633.

References

[1] P. Eilbracht, L. Bärfacker, C. Buss, C. Hollmann, B.E. Kitsos-Rzychon, C. L. Kranemann, T. Rische, R. Roggenbuck, A. Schmidt, Tandem reaction sequences under hydroformylation conditions: new synthetic applications of transition metal catalysis, Chem. Rev. 99 (1999) 3329–3366, https://doi.org/10.1021/cr970413r.

[2] M. Ahmed, A.M. Seayad, R. Jackstell, M. Beller, Amines made easily: a highly selective hydroaminomethylation of olefins, J. Am. Chem. Soc. 125 (2003) 10311–10318, https://doi.org/10.1021/ja030143w.

[3] M. Kraume, S. Enders, A. Drews, R. Schomäcker, S. Engell, K. Sundmacher, Integrated Chemical Processes in Liquid Multiphase Systems, De Gruyter, 2022.

[4] A. Behr, G. Henze, R. Schomäcker, Thermoregulated liquid/liquid catalyst separation and recycling, Adv. Synth. Catal. 348 (2006) 1485–1495, https://doi.org/10.1002/adsc.200606094.

[5] J.M. Dreimann, T.A. Faßbach, S. Fuchs, M.R.L. Fürst, T. Gaide, R. Kuhlmann, K. A. Ostrowski, A. Stadler, T. Seidensticker, D. Vogelsang, H.W.F. Warmeling, A. J. Vorholt, Vom Laborkuriosum zum kontinuierlichen Prozess: Die Entwicklung thermomorpher Lösungsmittelsysteme, Chemie Ingenieur Technik 89 (2017) 252–262, https://doi.org/10.1002/cite.201600119.

[6] J. Bianga, K.U. Künnemann, L. Goclik, L. Schurm, D. Vogt, T. Seidensticker, Tandem catalytic amine synthesis from alkenes in continuous flow enabled by integrated catalyst recycling, ACS Catal. 10 (2020) 6463–6472, https://doi.org/10.1021/acscatal.0c01465.

[7] J. Bianga, K.U. Künnemann, T. Gaide, A.J. Vorholt, T. Seidensticker, J. M. Dreimann, D. Vogt, Thermomorphic multiphase systems: switchable solvent mixtures for the recovery of homogeneous catalysts in batch and flow processes, Chemistry 25 (2019) 11586–11608, https://doi.org/10.1002/chem.201902154.
[8] M. Gerlach, S. Kirschtowski, A. Seidel-Morgenstern, C. Hamel, Kinetic modeling of the palladium-catalyzed isomerizing methoxycarbonylation of 1-decene, Chemie Ingenieur Technik 90 (2018) 673–678, https://doi.org/10.1002/cite.201700162.
[9] T. Gaide, J.M. Dreimann, A. Behr, A.J. Vorholt, Overcoming phase-transfer limitations in the conversion of lipophilic oleo compounds in aqueous media-a thermomorphic approach, Angew. Chem. Int. Ed. Eng. 55 (2016) 2924–2928, https://doi.org/10.1002/anie.201510738.
[10] A. Jörke, T. Gaide, A. Behr, A. Vorholt, A. Seidel-Morgenstern, C. Hamel, Hydroformylation and tandem isomerization–hydroformylation of n-decenes using a rhodium-BiPhePhos catalyst: kinetic modeling, reaction network analysis and optimal reaction control, Chem. Eng. J. 313 (2017) 382–397, https://doi.org/10.1016/j.cej.2016.12.070.
[11] M. Jokiel, N.M. Kaiser, P. Kováts, M. Mansour, K. Zähringer, K.D.P. Nigam, K. Sundmacher, Helically coiled segmented flow tubular reactor for the hydroformylation of long-chain olefins in a thermomorphic multiphase system, Chem. Eng. J. 377 (2019), 120060, https://doi.org/10.1016/j.cej.2018.09.221.
[12] K.H.G. Rätze, M. Jokiel, N.M. Kaiser, K. Sundmacher, Cyclic operation of a semi-batch reactor for the hydroformylation of long-chain olefins and integration in a continuous production process, Chem. Eng. J. 377 (2019), 120453, https://doi.org/10.1016/j.cej.2018.11.151.
[13] M. Gerlach, D. Abdul Wajid, L. Hilfert, F.T. Edelmann, A. Seidel-Morgenstern, C. Hamel, Impact of minor amounts of hydroperoxides on rhodium-catalyzed hydroformylation of long-chain olefins, Catal. Sci. Technol. 7 (2017) 1465–1469, https://doi.org/10.1039/c7cy00244k.
[14] S. Kirschtowski, F. Jameel, M. Stein, A. Seidel-Morgenstern, C. Hamel, Kinetics of the reductive amination of 1-undecanal in thermomorphic multicomponent system, Chem. Eng. Sci. 230 (2021), 116187, https://doi.org/10.1016/j.ces.2020.116187.
[15] W. Kortuz, S. Kirschtowski, A. Seidel-Morgenstern, C. Hamel, Kinetics of the rhodium-catalyzed hydroaminomethylation of 1-decene in a thermomorphic solvent system, Chemie Ingenieur Technik 94 (2022) 760–765, https://doi.org/10.1002/cite.202100180.
[16] V. Froidevaux, C. Negrell, S. Caillol, J.-P. Pascault, B. Boutevin, Biobased amines: from synthesis to polymers; present and future, Chem. Rev. 116 (2016) 14181–14224, https://doi.org/10.1021/acs.chemrev.6b00486.
[17] P. Kalck, M. Urrutigoïty, Tandem hydroaminomethylation reaction to synthesize amines from alkenes, Chem. Rev. 118 (2018) 3833–3861, https://doi.org/10.1021/acs.chemrev.7b00667.
[18] G. Kiedorf, D.M. Hoang, A. Müller, A. Jörke, J. Markert, H. Arellano-Garcia, A. Seidel-Morgenstern, C. Hamel, Kinetics of 1-dodecene hydroformylation in a thermomorphic solvent system using a rhodium-biphephos catalyst, Chem. Eng. Sci. 115 (2014) 31–48, https://doi.org/10.1016/j.ces.2013.06.027.
[19] S. Kirschtowski, C. Kadar, A. Seidel-Morgenstern, C. Hamel, Kinetic modeling of rhodium-catalyzed reductive amination of undecanal in different solvent systems, Chemie Ingenieur Technik 92 (2020) 582–588, https://doi.org/10.1002/cite.201900135.
[20] J. Markert, Y. Brunsch, T. Munkelt, G. Kiedorf, A. Behr, C. Hamel, A. Seidel-Morgenstern, Analysis of the reaction network for the Rh-catalyzed hydroformylation of 1-dodecene in a thermomorphic multicomponent solvent system, Appl. Catal. A Gen. 462-463 (2013) 287–295, https://doi.org/10.1016/j.apcata.2013.04.005.
[21] A. Jörke, S. Triemer, A. Seidel-Morgenstern, C. Hamel, Kinetic investigation exploiting local parameter subset selection: isomerization of 1-decene using a Rh-biphephos catalyst, Chemie Ingenieur Technik 87 (2015) 713–725, https://doi.org/10.1002/cite.201400148.
[22] F. Jameel, M. Stein, Solvent effects in hydroformylation of long-chain olefins, Mol. Catal. 503 (2021), 111429, https://doi.org/10.1016/j.mcat.2021.111429.
[23] D. Crozet, M. Urrutigoïty, P. Kalck, Recent advances in amine synthesis by catalytic hydroaminomethylation of alkenes, ChemCatChem 3 (2011) 1102–1118, https://doi.org/10.1002/cctc.201000411.
[24] T. Senthamarai, K. Murugesan, J. Schneidewind, N.V. Kalevaru, W. Baumann, H. Neumann, P.C.J. Kamer, M. Beller, R.V. Jagadeesh, Simple ruthenium-catalyzed reductive amination enables the synthesis of a broad range of primary amines, Nat. Commun. 9 (2018) 4123, https://doi.org/10.1038/s41467-018-06416-6.
[25] J.A. Fuentes, P. Wawrzyniak, G.J. Roff, M. Bühl, M.L. Clarke, On the rate-determining step and the ligand electronic effects in rhodium catalysed hydrogenation of enamines and the hydroaminomethylation of alkenes, Catal. Sci. Technol. 1 (2011) 431, https://doi.org/10.1039/c1cy00026h.
[26] F. Jameel, M. Stein, The many roles of solvent in homogeneous catalysis - the reductive amination showcase, J. Catal. 405 (2022) 24–34, https://doi.org/10.1016/j.jcat.2021.11.010.
[27] B. Hamers, E. Kosciusko-Morizet, C. Müller, D. Vogt, Fast and selective hydroaminomethylation using xanthene-based amino-functionalized ligands, ChemCatChem 1 (2009) 103–106, https://doi.org/10.1002/cctc.200900088.
[28] D. Crozet, C.E. Kefalidis, M. Urrutigoïty, L. Maron, P. Kalck, Hydroaminomethylation of styrene catalyzed by rhodium complexes containing chiral diphosphine ligands and mechanistic studies: why is there a lack of asymmetric induction? ACS Catal. 4 (2014) 435–447, https://doi.org/10.1021/cs400906b.
[29] C.J. Scheuermann Née Taylor, C. Jaekel, Enantioselective hydrogenation of enones with a hydroformylation catalyst, Adv. Synth. Catal. 350 (2008) 2708–2714, https://doi.org/10.1002/adsc.200800462.
[30] D. Crozet, A. Gual, D. McKay, C. Dinoi, C. Godard, M. Urrutigoïty, J.-C. Daran, L. Maron, C. Claver, P. Kalck, Interplay between cationic and neutral species in the rhodium-catalyzed hydroaminomethylation reaction, Chemistry 18 (2012) 7128–7140, https://doi.org/10.1002/chem.201103474.
[31] F.G. Helfferich, Kinetics of Multistep Reactions, secondnd ed., Elsevier, Amsterdam, Boston, 2004.
[32] D. Murzin, Catalytic Kinetics, Elsevier, Amsterdam, 2005.
[33] J.A. Christiansen, The Elucidation of Reaction Mechanisms by the Method of Intermediates in Quasi-Stationary Concentrations, Elsevier, 1953, pp. 311–353.
[34] S. Schlüter, K.U. Künnemann, M. Freis, T. Roth, D. Vogt, J.M. Dreimann, M. Skiborowski, Continuous co-product separation by organic solvent nanofiltration for the hydroaminomethylation in a thermomorphic multiphase system, Chem. Eng. J. 409 (2021), 128219, https://doi.org/10.1016/j.cej.2020.128219.
[35] F. Huxoll, A. Kampwerth, T. Seidensticker, D. Vogt, G. Sadowski, Predicting solvent effects on homogeneity and kinetics of the hydroaminomethylation: a thermodynamic approach using PC-SAFT, Ind. Eng. Chem. Res. 61 (2022) 2323–2332, https://doi.org/10.1021/acs.iecr.1c03891.
[36] S.-J. Chen, Y.-Q. Li, P. Wang, Y. Lu, X.-L. Zhao, Y. Liu, Promotion effect of water on hydroformylation of styrene and its derivatives with presence of amphiphilic zwitterionic phosphines, J. Mol. Catal. A Chem. 407 (2015) 212–220, https://doi.org/10.1016/j.molcata.2015.07.004.
[37] T. Oku, M. Okada, M. Puripat, M. Hatanaka, K. Morokuma, J.-C. Choi, Promotional effect of CH3I on hydroxycarbonylation of cycloalkene using homogeneous rhodium catalysts with PPh3 ligand, J. CO2 Utiliz. 25 (2018) 1–5, https://doi.org/10.1016/j.jcou.2018.02.015.